



Electrochemical Synthesis of Sodium Ferrate and Its Application in Wastewater Treatment Systems: A Field Case Study

A. P. Petkova^a, A. I. Konyashina^b, G. R. Sharafutdinova^{*a}

^a Empress Catherine II Saint Petersburg Mining University, Saint Petersburg, Russia

^b Dobrokhim LLC, Saint Petersburg, Russia

PAPER INFO

Paper history:

Received 08 April 2025

Received in revised form 24 May 2025

Accepted 09 June 2025

Keywords:

Sodium Ferrate

Electrochemical Process

Reactor

Consumable Anode

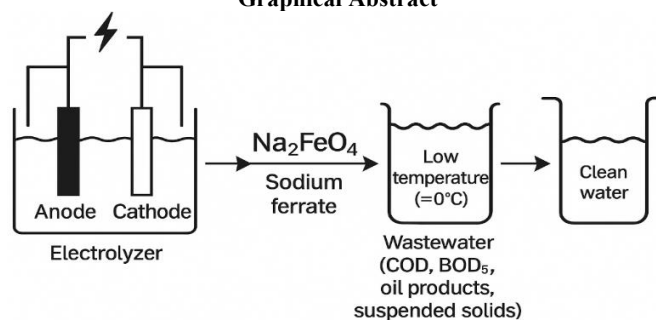
Electrolyte

ABSTRACT

A membrane reactor with an integrated flow-through photometric sensor was developed for real-time monitoring of sodium ferrate concentration. The materials for the reactor housing, sensor, and consumable anodes were selected, along with optimal electrolysis parameters that ensure increased ferrate yield and concentration, reduced energy consumption, and stable operation for up to 8 hours. The developed equipment and the produced reagent were tested on wastewater from oil extraction treatment facilities at the South Priobskoye field under Arctic conditions. At one site, ferrate was added directly to the wastewater with subsequent filtration; at another, it was used as part of an integrated treatment system including aeration and multi-stage filtration. Field trials demonstrated the high efficiency of sodium ferrate as an oxidant, coagulant, and flocculant: achieving degradation of organic and toxic compounds, removal of petroleum products, and water disinfection. Treated wastewater met regulatory standards and allowed safe discharge into the environment. The obtained results confirm the possibility of introduction of automated adaptive equipment for sodium ferrate synthesis into water treatment systems at oil production facilities. Utilizing sodium ferrate enhances treatment efficiency, lowers operating costs, and improves the environmental sustainability of production.

doi: 10.5829/ije.2026.39.02b.18

Graphical Abstract



1. INTRODUCTION

Biological treatment methods are effective in removing macro-pollutants (biodegradable organic substances, nitrogen, phosphorus, sulphur compounds, etc.) and low concentrations of trace metal ions (copper, iron,

manganese, etc.). However, these methods are not sufficiently effective for treating industrial and domestic wastewater containing persistent chemical compounds. Moreover, the elimination of bacteriological contamination requires the use of strong oxidizing agents (1-3). Modern research confirms the importance of

*Corresponding Author Email: s215102@stud.spmi.ru
(G. R. Sharafutdinova)

developing waste treatment methods aimed at reducing their environmental impact (4, 5). Therefore, the actual task is to search for cheap and environmentally safe technologies of wastewater treatment without chlorine-containing reagents, which are not inferior in efficiency and cost to the used technologies using hypochlorite (chlorine), as well as to solve the problem of fulfilling the requirements for wastewater purity in the absence of chlorine (6, 7).

In the treatment of domestic and industrial wastewater, alkali metal ferrate salts decompose toxic chemical compounds and petroleum products, eliminate microorganisms, and remove them from aqueous solutions through coagulation. Sodium ferrate is a universal reagent, which is successfully used for the purification of aqueous media from a variety of pollutants, including petroleum products, their derivatives, various fuels, nitrogen-, phosphorus- and sulphur-containing compounds, cyanides, ammonia and heavy metals (8-10). It is particularly effective at pollutant spillage sites, industrial wastewater and water bodies. The use of ferrate demonstrates high efficiency in removing toxic elements such as arsenic (As) and lead (Pb), and can also effectively address contamination caused by cobalt (Co), nickel (Ni), copper (Cu), and aluminum (Al) (11-13).

An important advantage of sodium ferrate is its ability to generate significantly less sludge compared to conventional coagulants such as ferrous sulfate, ferric nitrate, ferric chloride, and aluminum sulfate (14). This characteristic makes ferrate a more economically and environmentally favorable option for widespread application in water treatment.

Due to their high oxidation tendency, ferrates are subject to rapid degradation during storage or transport, which necessitates their direct production at the point of use. One of the most promising methods of sodium ferrate synthesis directly at the place of its application is membrane electrolysis. Membrane electrolysis in comparison with the nonseparated cell (15) provides a significant increase in productivity and reduction of energy consumption due to the prevention of ferrate decomposition on the cathode and flow production mode with the possibility of adaptive change of ferrate concentration in the solution by changing the current strength and the rate of electrolyte recirculation. In addition, the tightness of the cathode and anode chambers in the membrane electrolyzer prevents the interaction of hydrogen and oxygen by-products produced in them, thus minimising the risk of explosive mixtures.

In membrane electrolysis, within a reactor divided into cathode and anode chambers by a cation-exchange membrane, a steel consumable anode undergoes decomposition in an alkaline solution, leading to the formation of sodium ferrate (Na_2FeO_4) along with by-products such as oxygen and hydrogen (16, 17).

The concentration of ferrate in solution and anode passivation are influenced by the composition, concentration of electrolyte and its recirculation mode {Sun, 2018 #19;Petkova, 2024 #20;Quino-Favero, 2018 #21}. The electrolyte composition should ensure sufficient process productivity while minimizing energy consumption and production costs. This can be achieved by selecting the material of the consumable anode and the rate of catholyte (alkali-cure) supply synchronized with the rate of ferrate (anolyte) extraction. Recirculation of the anolyte in the anodic compartment contributes to an increase in ferrate concentration by promoting active mixing of the electrolyte and suppressing anode passivation. Therefore, the main objective of this study is to justify the optimal composition, concentration, and recirculation mode of the electrolyte in order to enhance the productivity, energy efficiency, and cost-effectiveness of the sodium ferrate electrolysis process.

An essential consideration for the efficiency of sodium ferrate electrochemical synthesis. The anode not only serves as a source of iron but also directly influences the reaction rate, product yield, and energy consumption of the process. It is essential to take into account the corrosion resistance of the anode material, as the aggressive conditions of electrolysis can significantly reduce its service life. Optimizing the composition and structure of anodes to enhance their electrochemical performance and increase durability remains a pressing challenge in current materials science research.

A major drawback of conventional methods used to control ferrate concentration in solution (such as potentiometric titration and spectrophotometry) is their inability to accurately determine ferrate concentration in the solution obtained during electrolysis without prior dilution by at least a factor of ten. In contrast, a key advantage of a flow sensor is its ability to monitor ferrate concentration in real time without the need for dilution.

It is also important to choose a design solution and manufacturing method for a scalable reactor vessel with a chamber with an integrated flow-through photocolometric sensor to determine the concentration of sodium ferrate in real time to ensure stable and safe production. Enhancing material efficiency and reducing operating costs are key considerations in the design of equipment for complex technical systems. These factors become particularly important in aggressive environments, where high structural reliability and durability are required (18-20).

Most studies utilize high-concentration NaOH solutions (40-60%) to increase ferrate yield, which results in higher energy consumption, increased risks associated with handling concentrated solutions, and alkalization of the treated water. Based on Russian literature, a 20% NaOH solution was selected as the electrolyte. Key electrolysis parameters identified for improving ferrate concentration, process efficiency, and

stability include current density, catholyte flow rate, anolyte recirculation rate, and the consumable anode material. The use of 20% NaOH reduces energy consumption but requires an increase in ferrate concentration to ensure effective performance at low dosages. This underscores the importance of optimizing synthesis parameters and consumable anode materials.

Taking the above into account, a research methodology was developed that includes the selection of materials and parameters for the electrochemical synthesis of sodium ferrate, the design of a flow-through membrane reactor, its fabrication using 3D printing technology, as well as laboratory and field testing of both the reactor and the sodium ferrate solution it produces. The effectiveness of the resulting reagent was evaluated in the treatment of real wastewater from facilities No. 40 and No. 150 at the Yuzhno-Priobskoye oil field, considering ferrate dosage, dosing mode, contaminant composition, and ambient temperature. A flowchart of the methodology is presented in Figure 1.

2. EXPERIMENTAL METHOD

The flow-through production of sodium ferrate was carried out in a membrane electrochemical reactor. A sodium hydroxide (NaOH) solution was chosen as the electrolyte due to its higher productivity compared to other electrolytes (21-23), which is attributed to better

dissolution of iron oxides/hydroxides and accelerated decomposition of the consumable anode. A 20% NaOH solution was used, which provided reduced electrical resistance, lower energy consumption during ferrate synthesis, and increased membrane durability compared to more concentrated solutions (35-40%) used in analogous systems. Higher alkali concentrations lead to an increase in ionic strength and, consequently, higher electrode overpotentials. This results in a rise in the overall cell operating voltage, especially at high current densities. Moreover, the risk of electrochemical degradation of the ion-exchange membrane increases due to intensified side reactions and the accumulation of aggressive intermediate products capable of damaging the polymer matrix and ion-exchange groups (24).

In the literature, materials such as Pt, Ti, Ni, Cu, and corrosion-resistant steels have been considered as cathodes. These materials demonstrated comparable performance, which allowed for the selection of the most cost-effective options (25). The cathodes were fabricated by laser cutting from the most affordable and readily available material resistant to alkali and sodium ferrate—08X18H9T austenitic stainless steel. A Nafion-324 cation-exchange membrane was selected for operation at the chosen alkali concentration (26).

Since a number of studies (15, 21) have shown that ferrate productivity increases in steels with a high silicon content—as well as in cast irons, which also contain silicon—electrical hot-rolled ferritic steel grade 1512, containing 4.5% silicon, was selected as the consumable anode material. For this type of steel, only the silicon content is regulated—ranging from 3.8 to 4.8%. These are low-carbon steels containing up to 0.05% C, which ensures a ferritic microstructure. The literature reports a positive effect of silicon in the range of 2–3% on increasing ferrate yield. A similar effect is observed for increased carbon content in steels compared to Armco iron. Steels and cast irons are commonly considered as materials for consumable anodes. In these materials, cementite decomposes in alkaline media faster than iron, thereby enhancing ferrate synthesis efficiency and reducing the rate of anode passivation. Anode passivation, caused by the formation of an oxide film on the surface, slows down or inhibits ferrate synthesis, leading to a gradual decrease in ferrate concentration, an increase in anodic voltage, and reduced process stability with respect to time. According to the literature, similar to carbon, silicon—present in electrical steels (2–3% Si) and transformer steels (3.8–4.8% Si)—reduces anode passivation. The presence of Si in solid solution within ferrite accelerates anode dissolution and ferrate formation. As the silicon content in the anode increases and intermediate silicate complexes form on its surface, selective oxidation contributes more significantly to anode dissolution, expansion of the active surface area, and increased porosity and permeability of the

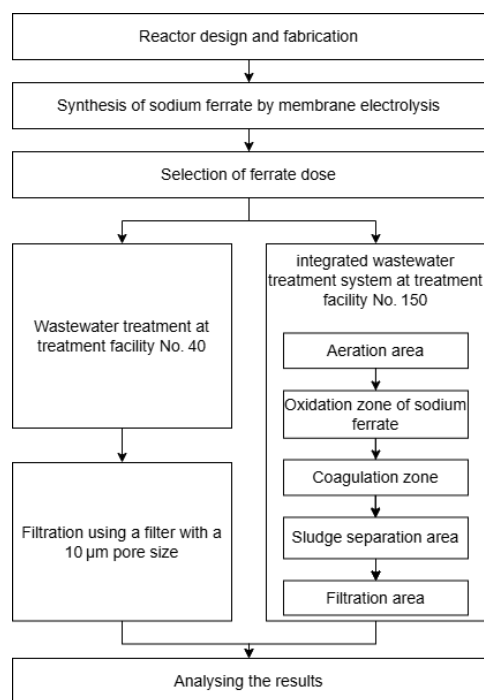


Figure 1. Flowchart of the methodology for the synthesis, application, and evaluation of sodium ferrate in wastewater treatment.

passivating oxide film. This selective dissolution of anodes leads to higher ferrate concentration in the solution, improved ferrate yield, and greater process stability with respect to time.

When selecting materials and manufacturing methods for the reactor housing, several options were considered: bonded acrylic housings, welded housings made from polypropylene sheets, and housings fabricated using 3D printing from polymers resistant to alkali and oxidizing agents that cause material aging and embrittlement. The drawbacks of bonded and welded housings include labor-intensive manufacturing, limited sealing reliability, and restrictions on reactor dimensions. To overcome these limitations, 3D printing was employed in the reactor housing design, allowing for the creation of scalable models with various capacities and configurations. The reactor housing was designed using KOMPAS-3D software and printed with a 3D printer (26). Polypropylene, known for its high chemical resistance to alkali and ferrate solutions at the target concentrations, was selected as the body material. The use of modern polymer materials ensures structural durability and resistance to aggressive environments—key factors for the efficient operation of the equipment (27). During the 3D printing process, shrinkage and deformation of the reactor body may occur due to uneven cooling rates between the upper and lower layers. Reinforcement of polypropylene filament with short glass fibers significantly reduces shrinkage and warping, while also enhancing the strength and stiffness of the printed part (28). Printing with unreinforced polypropylene filament results in significant shrinkage—up to 6% and warping of the reactor housing. In contrast, using glass fiber-reinforced polypropylene filament reduces shrinkage to as low as 0.2%. ABS housings, despite their low shrinkage, quickly become brittle due to aging under the influence of the oxidizing agent. The cost of PEEK filament, which offers excellent resistance to alkalis and oxidants, is approximately ten times higher than that of polypropylene filament. Therefore, glass fiber-reinforced polypropylene filament (Nova PPGF by Novaprint 3D) was selected for printing, as it provides high chemical resistance, mechanical strength, and minimal shrinkage (17). Printing was carried out using a Sapphire S 3D printer (TWO TREES) with a nozzle temperature of 270 °C, bed temperature of 95 °C, layer thickness of 0.2 mm, and nozzle diameter of 0.8 mm.

As the concentration of ferrate in the produced solution increases, the required dose of ferrate solution added to the treated water decreases proportionally. This enables a reduction in alkalinity and pH, while also allowing the treatment of more heavily contaminated wastewater with high COD and BOD levels, all while lowering alkali consumption and the overall cost of ferrate production (29, 30). To increase the concentration of sodium ferrate in solution, as well as to enhance

process productivity and duration, reactor design configurations and consumable anode compositions were selected to allow flexible adjustment of ferrate concentration, volume, and yield depending on the specific application conditions.

The reactor vessel, manufactured using 3D printing from reinforced polypropylene (Figure 2b), features grooves for securing membranes and electrodes. The arrangement of the anode and two cathode chambers, as well as the catholyte and anolyte supply system located in the bottom and side walls of the cell vessel, is similar to that of the previous version (Figure 2a). The reactor walls are 5 to 10 mm thick and include grooves for mounting the anodes (or anode frames), as well as the frames holding the membranes and cathodes. Channels for catholyte and anolyte recirculation are integrated into the bottom and side walls of the reactor vessel. Quick-release modular frames with clamps for attaching thin anodes, membranes, and cathodes were also fabricated using 3D printing from 3 mm thick polypropylene.

The side chamber for ferrate collection is equipped with a built-in compact flow photometric sensor for measuring ferrate concentration in the alkaline solution. On the left side, a wall section is designated for mounting peristaltic pumps onto the reactor body. Camozzi polypropylene fittings with EPDM seals, installed in the bottom and side chambers of the reactor vessel, securely connect fluoroplastic tubes of the circulation circuit used for alkali supply and ferrate extraction.

On the left side, a wall section is provided for mounting peristaltic pumps directly onto the reactor body. Camozzi polypropylene fittings with EPDM seals, screwed into the bottom and side chamber of the cell housing, secure fluoroplastic tubing of the circulation circuit for feeding alkali and discharging the ferrate solution.

The reactor is equipped with two peristaltic pumps mounted directly on its body, which operate synchronously to supply and discharge the electrolyte.

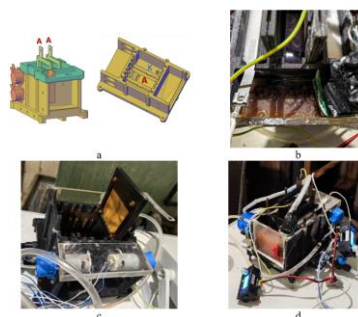


Figure 2. Layout of the flow-through reactor: a – 3D model; b – reactor vessel made of fiberglass-reinforced polypropylene; c – frame for securing the membrane and cathodes; d – flow photometric sensor for sodium ferrate concentration monitoring

One pump feeds alkali into the cathode chambers, from where it overflows into the anode chamber. The ferrate solution then flows into a side chamber equipped with a concentration sensor and is subsequently returned to the anode chamber by the second pump. Continuous recirculation of ferrate through the anode chamber eliminates diffusion limitations on the electrode surface and prevents the formation of an oxide film.

The stability of ferrate concentration in the solution is ensured by selecting a recirculation rate at which ferrate decomposition does not exceed its generation. With proper adjustment of the electrolyte feed rate, the ferrate concentration in the solution increases, and productivity with recirculation can rise from 55% to 80–90% (31).

The design and appearance of the frame for securing the membrane and cathodes are shown in Figure 3a. The 0.5 mm thick transformer steel anode was inserted into a detachable frame composed of two 3 mm thick parts. The housings of the cell, sensor, and frames for the anode and membrane were fabricated using 3D printing from glass fiber-reinforced polypropylene resistant to alkali and ferrate.

The flow-through photometric sensor enables direct analysis of sodium ferrate solution without dilution by shortening the optical path length through appropriate selection of cuvette width (ranging from 2 to 0.5 mm) and using sufficiently powerful laser light sources. The concentration of ferrate is proportional to the change in optical density at 510 nm, which corresponds to the absorption maximum of sodium ferrate solutions. The compact flow-through sensor incorporates two laser sources in the green and red spectral ranges and a miniature flow cell made of quartz glass with a width of 0.5 mm. The sensor housing was also fabricated via 3D printing using glass fiber-reinforced polypropylene.

The flow-through photometric sensor was calibrated using a calibration curve obtained with a spectrophotometer at an optical path length of $l = 1$ cm (20). The zero optical density reference was taken as the value measured for a 20% NaOH solution. A freshly prepared sodium ferrate solution, when measured without prior dilution, completely absorbs visible light. To construct the calibration curve (Figure 2a), a series of sodium ferrate solutions was prepared by diluting the stock solution by at least a factor of 10, and each

subsequent dilution was made at a twofold ratio relative to the previous one. An absorption peak characteristic of ferrate (VI) solutions was identified at a wavelength of 510 nm. The ferrate concentration was calculated using the formula $C = A/(\varepsilon \cdot l)$, where ε is the molar absorption coefficient ($\varepsilon_{510\text{nm}} = 1150 \pm 25 \text{ M}^{-1} \cdot \text{cm}^{-1}$), l is the optical path length ($l = 1$ cm), and A is the absorbance, ranging from 0 to 1.14. For more concentrated sodium ferrate solutions whose absorbance exceeded the upper limit of the calibration curve, the dilution factor was adjusted experimentally (15-fold, 20-fold, 25-fold, etc.) to bring the values within the calibrated range. The resulting concentrations were then recalculated based on the dilution factor and stored in the device's memory. Since the flow-through sensor is calibrated based on analytically determined concentrations, this affects the accuracy of real-time concentration measurements. The results obtained by spectrophotometry at 510 nm and by the flow-through photometric sensor showed satisfactory agreement, with deviations within 10%. The compact built-in sensor enables determination of sodium ferrate concentrations up to 10 g/L, while significantly reducing the size and cost of the measurement system.

The relevance of testing sodium ferrate at the treatment facilities of the Yuzhno-Priobskoye oil field, which are biological treatment stations, is due to the growing annual load on these facilities and the need to remove chemical, biological, and bacterial contaminants and microorganisms to meet maximum permissible concentration (MPC) standards.

To assess the efficiency of wastewater treatment with sodium ferrate solution, samples of biologically treated wastewater were taken from wastewater treatment facilities No. 40 and No. 150. The initial and final water quality parameters are presented in Table 1. The analysis of wastewater samples before and after treatment with sodium ferrate was carried out in an accredited laboratory in accordance with Russian national standards corresponding to internationally recognized methods. Suspended solids were determined gravimetrically (PND F 14.1:2:4.254-09), equivalent to APHA SM 2540 D. Hardness was measured titrimetrically (PND F 14.1:2:3.98-97), similar to APHA SM 2340 C. Petroleum hydrocarbons were analyzed fluorimetrically (PND F 14.1:2:4.128-98), partially corresponding to EPA 442.0. Biochemical oxygen demand (BOD₅) was determined amperometrically (PND F 14.1:2:3:4.123-97), analogous to APHA SM 5210 B. Chemical oxygen demand (COD) was measured using the dichromate method (GOST 31859), corresponding to ISO 6060 and APHA SM 5220 C. pH was measured electrometrically (PND F 14.1:2:3:4.121-97), equivalent to APHA SM 4500-H⁺ B. Color was determined on the platinum-cobalt scale according to GOST 31868-2012 (Method B), similar to APHA SM 2120 C. Bicarbonates were calculated based on total alkalinity according to GOST 31957 Method A,



Figure 3. Quick-release assembly frames: a – frame for securing the cathode with membrane; b – frame for securing the 0.5 mm thick anode

consistent with Standard Methods practices. Thermotolerant coliform bacteria (CFU/100 mL) were determined using membrane filtration and incubation at elevated temperature ($44 \pm 0.5^\circ\text{C}$) following MUK 4.2.1018-01, analogous to APHA SM 9221 E. Coliphages were detected using the double-layer agar method with *E. coli* CN-13, in accordance with MUK 4.2.1884-04, corresponding to ISO 10705-1 and APHA SM 9224 B. Hydrogen sulfide and sulfides were measured photometrically using methylene blue according to PND F 14.1:2:4.63-96. The method is based on the reaction of hydrogen sulfide with reagents in acidic medium followed by photometric detection, equivalent to APHA SM 4500-S²⁻ D. Mineralization (total dissolved solids) was determined gravimetrically

TABLE 1. Initial composition of wastewater before treatment with sodium ferrate (Sources No. 40 and No. 150)

Parameter	Before treatment wastewater treatment facility No. 40)	Before treatment wastewater treatment facility No. 150)	MPC
Suspended solids, mg/dm ³	175	236	12
Total hardness, °Ж	12,9	11,1	MPC: 7–10 for water; not regulated for wastewater
Petroleum hydrocarbons, mg/dm ³	0,271	0,78	<0,1
Total coliform bacteria, CFU/100 cm ³	30000	400000	<500
Thermotolerant coliform bacteria, CFU/100 cm ³	30000	400000	<100
Coliphages, PFU/100 cm ³	20	1000	<10
COD (Chemical Oxygen Demand), mgO ₂ /dm ³	445	650	<30
Bicarbonates, mg/dm ³	565	Not measured	<400
pH	8,7	8,5	6,5-8,5
Sulfides, mg/dm ³	0,071	Not measured	<1,5
Hydrogen sulfide, mg/dm ³	0,076	30	<0,05
BOD ₅ (Biochemical Oxygen Demand), mgO ₂ /dm ³	151	230	<4
Mineralization, mg/dm ³	470	790	<1000

according to PND F 14.1:2:4.261-10, similar to APHA SM 2540 C.

During dosing adjustment for continuous treatment of wastewater from wastewater treatment facility No. 150 using sodium ferrate solution, a preliminary ferrate concentration of 10 mg/L was established in the storage tank. Based on the plant's throughput of 100 L/h, this dose was recalculated for delivery once every 3 minutes. Sodium ferrate was dosed into the reaction column in an amount of 50 mg, corresponding to 5 L of flowing water over 3 minutes, using a chemically resistant membrane pump. At various stages of purification, pH was monitored, and in addition to color and turbidity, the presence and quantity of sediment on a cotton filter after effluent filtration were evaluated.

Field tests conducted at the Yuzhno-Priobskoye treatment facilities at an ambient temperature of around 0 °C enabled evaluation of the efficiency and stability of sodium ferrate solutions under low-temperature conditions and provided recommendations for the application of the reactor and produced reagent at wastewater treatment plants of oil wells in the Far North. Adaptive approaches aimed at increasing system performance and equipment efficiency are essential for achieving stable results, particularly in harsh climates and under seasonal environmental changes (32-34).

An experiment was conducted to determine the optimal dose of sodium ferrate solution for the treatment of biologically treated wastewater from treatment facility No. 40. Samples of wastewater were placed into five identical containers with a volume of 120 mL each (Figure 4a). Sodium ferrate solution was added to four of the containers in varying doses: 1.2 mg (Container No. 5), 1.8 mg (Container No. 4), 2.4 mg (Container No. 3), and 3.0 mg (Container No. 2). Container No. 1 served as the control and contained only biologically treated wastewater without any sodium ferrate added. In container No. 5, the addition of 1.2 mg of ferrate resulted in visible sediment formation within 5 minutes, along with a significant reduction in turbidity and color; the pH reached approximately 10. In container No. 4, where the dose was 1.8 mg, clear coagulation and intensive precipitation of organic matter were observed; the pH rose to 10. In container No. 3, after the addition of 2.4 mg of ferrate, the lowest color level was achieved. The amount of sediment remained almost unchanged, but the pH exceeded 10. In container No. 2, with a 3.0 mg dose, the excessive iron content caused yellowing of the water, indicating an overdosage of sodium ferrate.

The effective dose of sodium ferrate was determined to be 2.4 mg per 120 mL of wastewater (container No. 3), equivalent to 20 mg of ferrate per 1 liter of effluent. After treatment with sodium ferrate, the resulting sludge (Figures 3a and 3c) was filtered through a cotton filter (Figure 3b). In the image, the leftmost container contains

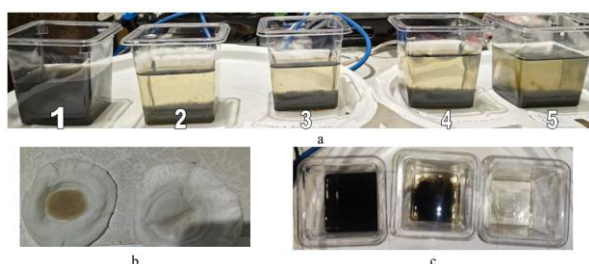


Figure 4. Selection of sodium ferrate dose: a – experimental setup for dose selection; b – filter cake after sedimentation; c – filtered water sample compared to original water

the untreated sample, the second shows sediment settled at the bottom, and the third illustrates the result of filtration through a cotton disk performed 2 minutes after ferrate addition, when floc formation had begun (Figure 3c). The large flocs formed settle completely, producing a loose sediment that can be easily removed using mechanical filters (with a filtration rating of 10–50 μm) or sorbents. Increasing holding time did not affect the water's color and turbidity. For surface waters, acceptable color values range from 30 to 90°. The color of the treated sample (Figure 6c) was approximately 40° on the platinum-cobalt scale, which meets the requirements for both surface and drinking water. Sample No. 3 also demonstrated a high level of clarity, indicating a minimal amount of suspended solids remaining after ferrate treatment.

To treat more heavily polluted wastewater from wastewater treatment facility No. 150 of the Yuzhno-Priobskoye oil field, a test filtration cycle was carried out on a pilot integrated treatment unit (Figure 5a). The unit consists of a sodium ferrate synthesis reactor and three connected columns: an aeration column with a filtration-oxidation block, a reaction column, and a sorption-filtration column. The water to be treated is first fed into the primary aeration column, then into the reaction column (Figure 5a). Sodium ferrate is produced in the electrochemical reactor (Figure 5b) and delivered to the reaction column by a chemically resistant membrane pump. The flocs formed from the contaminants settle at the bottom of the column, while the treated water flows into the third column. This final column contains a sorption filter, which captures any suspended solids not removed in the previous step and adjusts the pH of the treated water.

Wastewater from equalization overflow tanks (taken from the level below the foam and grease layer and above the sediment) is fed under pressure into Zone 1 at the top of the unit, where it is intensely saturated with oxygen from air supplied through process nozzles (Figure 6c). The aerated water flows downward along the inner contour of the tank and enters the coagulation zone (Zone 2), where, due to chemical reactions with oxygen, primary purification takes place—dissolved substances

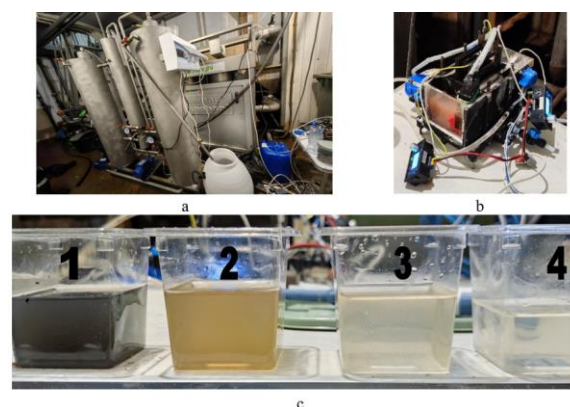


Figure 5. Integrated wastewater treatment plant: a – general view of the treatment system; b – sodium ferrate synthesis reactor; c – treated wastewater at different stages: 1 – initial untreated wastewater; 2 – during the first treatment stage; 3 – after treatment with ferrate; 4 – after passing through a mechanical filter at the outlet

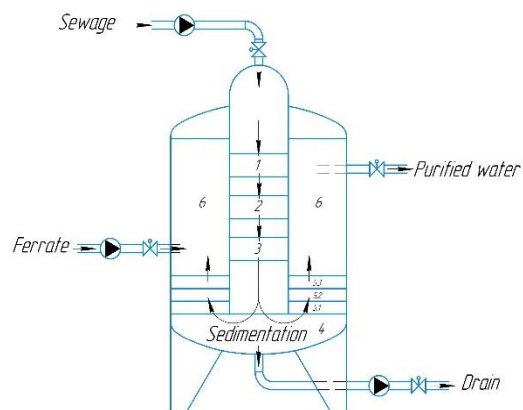


Figure 6. Schematic diagram of the pilot wastewater treatment unit with sequential zones for aeration (1), coagulation (2), ferrate treatment (3), sedimentation (4), multilayer filtration (5.1–5.3), and accumulation of purified water (6)

(salts, metals, etc.) are converted into insoluble forms, resulting in the formation of flocculent aggregates (sludge). The water then enters Zone 3, where it is treated with sodium ferrate at a dose of 10 mg/L. In this zone, the reagent reacts with contaminants, after which the water flows into the lower part of the unit—Zone 4, the settling zone—where flocculent aggregates, suspended solids, and mechanical impurities settle under the influence of gravity and are separated from the water. The clarified water then flows into the outer contour of the tank via communicating vessels and enters Zone 5, the filtration zone, where it is further purified using a multilayer filter bed (composed of 1 to 5 types of filtration media, layered accordingly).

A three-layer filtration media was used, consisting of activated sorbent (AC, 5.1) for the removal of iron and

manganese; modified sorbent (MC, 5.2) for the removal of iron, manganese, and hydrogen sulfide; and zeolite (5.3) for the elimination of nitrogen compounds and other contaminants from the wastewater. The water flows through the filtration media in Zone 5 in an upward direction, which also ensures effective retention of flocculent aggregates and suspended solids in the lower part of the unit. After passing through the filtration zone, the purified water enters Zone 6, the accumulation zone, located at the top of the outer contour of the system.

Samples obtained after the comprehensive treatment of wastewater from wastewater treatment facility No. 150 using sodium ferrate solution are shown in Figure 4. The color of sample No. 4 (Figure 4) after treatment is approximately 25° on the platinum-cobalt color scale, which meets the requirements for both surface and drinking water. Sample No. 4 also exhibits high transparency, indicating a very low concentration of suspended particles remaining after comprehensive treatment with sodium ferrate.

3. RESULTS AND DISCUSSION

The developed flow-through reactor with an integrated photometric sensor demonstrated stable operation and a high sodium ferrate yield under optimized conditions. Electrolysis was carried out in a 20% NaOH solution at a current density of 500 A/m² and a recirculation rate of 5.5 mL/min. These parameters ensured an average ferrate concentration of 5 g/L, a current efficiency of approximately 70%, and an energy consumption of 4.6 kWh/kg. Anodes made of transformer-grade ferritic steel 1512, containing up to 4.8% silicon, promoted the formation of silicate complexes and selective dissolution, which increased the anode's active surface area and ensured long-term process stability.

Field testing of the reactor and the resulting ferrate solution was conducted on wastewater from treatment facilities No. 40 and No. 150 of the Yuzhno-Priobskoye oil field under harsh Arctic climate conditions. At facility No. 40, ferrate was dosed directly into the wastewater, followed by filtration through a 10 µm pore-size filter. At facility No. 150, ferrate was used as part of an integrated treatment unit that included preliminary aeration and filtration through a three-layer bed of activated sorbent (AC), modified sorbent (MC), and zeolite, providing removal of Fe, Mn, H₂S, nitrogen compounds, and other contaminants. The use of an air–water mixture and the collision of liquid flows intensified oxidation, reduced reagent consumption, and simplified the system compared to mechanical mixing. Aeration lowered the pH, pre-oxidized contaminants, and generated microbubbles that served as nucleation sites for floc formation, thereby enhancing the coagulating effect of ferrate and reducing the required dosage. Counter-current

filtration enabled sludge concentration in the lower layers of the bed, increased filtration efficiency, and extended the backwashing interval.

Table 2 presents the results of wastewater treatment using sodium ferrate solution at wastewater treatment facilities No. 40 and No. 150. A dose of 20 mg/L was applied for treatment at facility No. 40, while at facility No. 150, a dose of 10 mg/L was used, delivered in 50 mg portions every 3 minutes with a treatment unit capacity of 100 L/h. The post-treatment parameters are compared with the maximum permissible concentrations (MPC) established for surface water, enabling an assessment of the feasibility of discharging treated wastewater onto soil or into open water bodies.

At facility No. 40, the suspended solids concentration decreased from 175 to 9.4 mg/L, below the MPC of 12 mg/L set by the Khanty-Mansiysk Vodokanal. The content of petroleum products dropped from 0.271 to 0.042 mg/L, well below the MPC (<0.1 mg/L). Total hardness reached 11.3 °dH, slightly exceeding the standard for surface waters (<10 mg/L); however, this parameter is not regulated for wastewater. The pH of the treated water was 8.5, which complies with the limits for domestic wastewater discharge.

For wastewater with high initial alkalinity or elevated COD and BOD₅ values, it is recommended to increase the ferrate concentration while proportionally decreasing the dosage volume, allowing for a reduction in final alkalinity and pH.

At both facilities, microbiological indicators met the sanitary standards. According to SanPiN 2.1.5.980-00, surface water should contain no more than 500 CFU/100 mL of total coliform bacteria (TCB), 100 CFU/100 mL of thermotolerant coliform bacteria (FCB), and 10 PFU/100 mL of coliphages. After treatment, all these indicators were below the permissible thresholds.

COD and BOD₅ values were below MPCs for recreational surface waters. Sulfide and bicarbonate concentrations were significantly lower than drinking water standards. Hydrogen sulfide levels after ferrate treatment were 16 times lower than the drinking water limit of 0.05 mg/L (SanPiN 1.2.3685-21). Mineralization was 2.5 to 3 times lower than the MPC of 1000 mg/L for drinking water.

The results for wastewater from facility No. 150 confirmed high treatment efficiency under low temperatures, with suspended solids reduced to 1.36 mg/L, petroleum products to nearly half the MPC, and hardness levels matching those of soft drinking water (≤3 °dH). The pH remained stable at 7.9, and all other parameters complied with regulatory standards.

In conclusion, sodium ferrate treatment proved effective at both wastewater treatment facilities. The treated effluent meets all regulatory criteria for discharge into open water bodies or onto soil. The stability and

TABLE 2. Wastewater quality after treatment with sodium ferrate at wastewater treatment facilities No. 40 and No. 150

Parameter	After treatment (wastewater treatment facility No. 40)	After treatment (wastewater treatment facility No. 150)	MPC
Suspended solids, mg/dm ³	9,4	1,36	12
Total hardness, °Ж	11,3	1,92	MPC: 7–10 for water; not regulated for wastewater
Petroleum hydrocarbons, mg/dm ³	0,042	0,053	<0,1
Total coliform bacteria, CFU/100 cm ³	250	250	<500
Thermotolerant coliform bacteria, CFU/100 cm ³	100	80	<100
Coliphages, PFU/100 cm ³	0	0	<10
COD (Chemical Oxygen Demand), mgO/dm ³	20	20	<30
Bicarbonates, mg/dm ³	10	Not measured	<400
pH	8,5	7,9	6,5-8,5
Sulfides, mg/dm ³	0,062	Not measured	<1,5
Hydrogen sulfide, mg/dm ³	0,003	0,0005	<0,05
BOD ₅ (Biochemical Oxygen Demand), mgO ₂ /dm ³	2,0	2,5	<4
Mineralization, mg/dm ³	400	350	<1000

efficiency of the ferrate reagent under low-temperature conditions confirm its suitability for use in the oil industry.

A similar methodology was applied for the treatment of toxic wastewater from the Red Bog hazardous waste landfill in Saint Petersburg using sodium ferrate. The reagent was synthesized in a laboratory reactor using 20% NaOH, with a feed rate of 4 mL/min, ferrate concentration of 6 g/L, current density of 500 A/m², and operating temperature of 30–45 °C. Sodium ferrate solution was used to treat industrial wastewater from storm runoff and from acidic lagoons No. 59, 66, and 67 at the site. For highly polluted lagoon waters with

elevated COD and BOD values, the optimal ferrate dose was determined based on changes in turbidity, color, pH, and sediment volume. For less contaminated stormwater, ferrate was applied as part of an integrated treatment system with oxidation, settling, and filtration chambers. The ferrate dose and flow rate were optimized during trial filtration cycles at a flow rate of 12–24 L/h.

The multilayer filtration media included activated sorbent (AC), modified sorbent (MC), and the ion-exchange sorbent Batlek. Regulatory limits for domestic wastewater were met for lagoon waters at ferrate doses of 50–60 mg/L, and for stormwater after oxidation with doses of 10–20 mg/L, at treatment capacities of 12 and 24 L/h depending on pollution level. In lagoon waters No. 64 and 68, cadmium concentrations were reduced by a factor of 2000 and lead by a factor of 100 at a ferrate dose of 100 mg/L, meeting discharge standards. These results confirmed the high efficiency of sodium ferrate in treating toxic industrial wastewater.

4. CONCLUSION

According to the proposed methodology, sodium ferrate can be used both for direct dosage optimization and as part of an integrated treatment system. The solution acts as a powerful oxidant, coagulant, and flocculant. Its effective disinfectant dose is significantly lower than those required by alternative methods, while the resulting by-products are environmentally safe. Ferrate (VI) compounds degrade toxic chemicals and petroleum products and eliminate microorganisms. In the oil industry, automated and adaptive ferrate production systems show promise for wastewater treatment and water reuse applications. For wastewater with high COD and BOD values, higher ferrate doses are required, highlighting the relevance of developing anode compositions that enable increased ferrate concentration in the solution while maintaining current efficiency, energy consumption, and process stability for up to 8 hours (a typical work shift interval between anode replacements).

At the selected treatment facilities in oil fields, ferrate dosage was determined based on changes in turbidity, color, pH, and sediment volume. The average capacity of the integrated treatment system is 100 L/h and can be adjusted according to pollution levels. The system consists of two identical modules (M1 and M2), as shown in Figure 6, which allows either doubling the flow rate or conducting additional treatment in module M2 using significantly lower ferrate doses (~0.5 mg/L) to meet turbidity and color standards. Ferrate was introduced via a dosing pump at 50 mg every 3 minutes, corresponding to a solution concentration of 10 mg/L.

According to the obtained data, the treated wastewater meets all regulatory limits for discharge into

soil and surface water bodies. Considering that the tests were conducted at ambient temperatures around 0 °C, the results confirm the high efficiency and stability of sodium ferrate solutions under low-temperature conditions. The field trials conducted at treatment facilities for oil production in the Russian Far North demonstrate the feasibility of deploying automated, adaptive ferrate production units and support the wide-scale use of sodium ferrate in the oil industry for wastewater treatment and water reuse.

The research was carried out within the state assignment of Ministry of Science and Higher Education of the Russian Federation (FSRW-2023-0002).

5. REFERENCES

- Dutta D, Arya S, Kumar S. Industrial wastewater treatment: Current trends, bottlenecks, and best practices. *Chemosphere*. 2021;285:131245. 10.1016/j.chemosphere.2021.131245
- Mao G, Han Y, Liu X, Crittenden J, Huang N, Ahmad UM. Technology status and trends of industrial wastewater treatment: A patent analysis. *Chemosphere*. 2022;288:132483. 10.1016/j.chemosphere.2021.132483
- Карапетян КГ, Дорош ИВ, Згонник ПВ, Коршунов АД, Перина АИ. Sorbents based on foamed phosphate glass for collecting petroleum oil products from contaminated soils and water surfaces. *Bulletin of the Tomsk Polytechnic University Geo Assets Engineering*. 2024;335(8):227-40. 10.18799/24131830/2024/8/4484
- Munyengabe A, Zvinowanda C, Ramontja J, Zvimba JN. Effective desalination of acid mine drainage using an advanced oxidation process: Sodium ferrate (VI) salt. *Water*. 2021;13(19):2619. 10.3390/w13192619
- Piirainen V, Mikhailov A, Barinkov V, Starovoitov V. The use of sludge-peat composition for the processing of alu-mina production waste. *Obogashchenie Rud*. 2022(6):51-8. 10.17580/or.2022.06.09
- Hassan K, Khalifa A, Hegazy M, Helmy M. Evaluation of an Outdoor Pilot Scale Hybrid Growth Algal-Bacterial System for Wastewater Bioremediation. *Civil Engineering Journal*. 2024;10(11):3589-602. 10.28991/CEJ-2024-010-11-09
- Perez OFA, Navarro AMS, Cardenas LA, Castellanos J, Velasquez P. Optimizing Cr (VI) reduction in plastic chromium plating wastewater: particle size, irradiation, titanium dose. *Emerging Science Journal*. 2024;8(1):17-27. 10.28991/ESJ-2024-08-01-02
- Alibabaei F, Saebnoori E, Fulazzaky MA, Talaiekhazani A, Roohi P, Moghadas F, et al. An evaluation of the efficiency of odorant removal by sodium ferrate (VI) oxidation. *Measurement*. 2021;179:109488. 10.1016/j.measurement.2021.109488
- Sarkheil H, Azimi Y, Rahbari S. Fuzzy wastewater quality index determination for environmental quality assessment under uncertain and vagueness conditions. *International Journal of Engineering*. 2018;31(8):1196-204. 10.5829/ije.2018.31.08b.06
- Altynbayeva G, Kadnikova O, Aydarhanov A, Toretayev M. Industrial Wastewaters of the Feed Industry: Use of Sodium Ferrate in the Phenol Purification Process. *Rigas Tehniskas Universitates Zinatniskie Raksti*. 2021;25(1):829-39. 10.2478/rtuct-2021-0062
- Sailo L, Pachuan L, Yang JK, Lee SM, Tiwari D. Efficient use of ferrate (VI) for the remediation of wastewater contaminated with metal complexes. *Environmental Engineering Research*. 2015;20(1):89-97. 10.4491/eer.2014.079
- Liu J, Muleños MR, Hockaday WC, Sayes CM, Sharma VK. Ferrate (VI) pretreatment of water containing natural organic matter, bromide, and iodide: A potential strategy to control soluble lead release from PbO₂ (s). *Chemosphere*. 2021;263:128035. 10.1016/j.chemosphere.2020.128035
- Munasir N. LR, Diah Hari K., Nuhaa F., Ezza S.S. . Synthesis of Fe₃O₄/SiO₂/PEG nanocomposite from mineral sands: Kinetic adsorption of heavy metal ion from aqueous solution. *International Journal of Engineering Transactions B: Applications*. 2025;38(2):330–42. 10.5829/ije.2025.38.02b.07
- Dong S, Mu Y, Sun X. Removal of toxic metals using ferrate (VI): a review. *Water Science and Technology*. 2019;80(7):1213-25. 10.2166/wst.2019.376
- Feihu Z, Sy Yi S. Electrochemical Synthesis of Ferrate (VI): Factors Influencing Synthesis and Current Research Trends. *Journal of Advanced Research in Applied Mechanics*. 2024;117(1):72-90. 10.37934/aram.117.1.7290
- Rai PK, Lee J, Kailasa SK, Kwon EE, Tsang YF, Ok YS, et al. A critical review of ferrate (VI)-based remediation of soil and groundwater. *Environmental research*. 2018;160:420-48. 10.1016/j.envres.2017.10.016
- Ghernaout D, Naceur M. Ferrate (VI): In situ generation and water treatment—A review. *Desalination and Water Treatment*. 2011;30(1-3):319-32. 10.5004/dwt.2011.2217
- Tiwari D. Ferrate (VI) a greener solution: Synthesis, characterization, and multifunctional use in treating metal-complexed species in aqueous solution. *Ferrites and Ferrates: Chemistry and Applications in Sustainable Energy and Environmental Remediation: ACS Publications*; 2016. p. 161-220.
- Yates BJ, Zboril R, Sharma VK. Engineering aspects of ferrate in water and wastewater treatment—a review. *Journal of Environmental Science and Health, Part A*. 2014;49(14):1603-14. 10.1080/10934529.2014.950924
- Korogodin A, Ivanov S. Assessment of the journal bearing health status in a drum mill used as a part of arctic complex mining equipment. 10.30686/1609-9192-2024-6-144-151
- Diaz M, Doederer K, Keller J, Cataldo M, Donose B-C, Ali Y, et al. Towards in situ electro-generation of ferrate for drinking water treatment: A comparison of three low-cost sacrificial iron electrodes. *Journal of Electroanalytical Chemistry*. 2021;880:114897. 10.1016/j.jelechem.2020.114897
- Barışçi S, Ulu F, Särkkä H, Dimoglo A, Sillanpää M. Electrosynthesis of ferrate (VI) ion using high purity iron electrodes: Optimization of influencing parameters on the process and investigating its stability. *International Journal of Electrochemical Science*. 2014;9(6):3099-117. 10.1016/S1452-3981(23)07995-6
- Deng Y, Guan X. Unlocking the potential of ferrate (VI) in water treatment: Toward one-step multifunctional solutions. *Journal of Hazardous Materials*. 2024;464:132920. 10.1016/j.jhazmat.2023.132920
- Han H, Li J, Ge Q, Wang Y, Chen Y, Wang B. Green ferrate (VI) for multiple treatments of fracturing wastewater: Demulsification, visbreaking, and chemical oxygen demand removal. *International journal of molecular sciences*. 2019;20(8):1857. 10.3390/ijms20081857
- Ding L. Removal of methyl mercaptan from foul gas by in-situ production of ferrate (VI) for odour control. 2013.
- Petkova AP, Gorbatyuk SM, Sharafutdinova GR, Nagovitsyn VA. Selection of materials and technologies for the electrochemical synthesis of sodium ferrate. *Metallurgist*. 2024;68(3):449-59. 10.1007/s11015-024-01747-w

27. Pryakhin E, Azarov V. Comparative analysis of the use of epoxy and fluoroplastic polymer compositions as internal smooth coatings of the inner cavity of steel main gas pipelines. 2024. 10.17580/cisr.2024.02.16
28. Shulga E, Karamov R, S. Sergeichev I, D. Konev S, I. Shurygina L, S. Akhatov I, et al. Fused filament fabricated polypropylene composite reinforced by aligned glass fibers. Materials. 2020;13(16):3442. 10.3390/ma13163442
29. Quino-Favero J, Eyzaguirre R, Mogrovejo P, Prieto P, del Pino LF. Electrochemical synthesis of ferrate (VI): optimization of parameters and evaluation of their impact in production cost. Desalination and Water Treatment. 2018;113:179-86. 10.5004/dwt.2018.22262
30. Azizifard A, Arkat J, Farughi H. Sustainable surface water management and wastewater treatment plant location: A case study of Urmia lake. International Journal of Engineering Transactions A: Basics 2020;33(4):621-30. 10.5829/ije.2020.33.04a.13
31. Alsheyab M, Jiang J-Q, Stanford C. On-line production of ferrate with an electrochemical method and its potential application for wastewater treatment—A review. Journal of Environmental Management. 2009;90(3):1350-6. 10.1016/j.jenvman.2008.10.001
32. Mikhailov A, Shibano D, Bessonov A, Bouguebrine C. Comprehensive Assessment Production Efficiency of Electric Rope Shovel through Operator Qualification Criteria. International Journal of Engineering Transactions A: Basics. 2024;37(07):1231. 10.5829/IJE.2024.37.07A.03
33. Litvinenko VS, Dvornikov MV, Trushko VL. Elaboration of a conceptual solution for the development of the Arctic shelf from seasonally flooded coastal areas. International Journal of Mining Science and Technology. 2022;32(1):113-9. 10.1016/j.ijmst.2021.09.010
34. Bazhin VY, Ustinova YV, Fedorov SN, Shalabi MEK. Improvement of energy efficiency of ore-thermal furnaces in smelting of aluminosilic raw materials. Записки Горного института. 2023(261 (eng)):384-91.

COPYRIGHTS

©2026 The author(s). This is an open access article distributed under the terms of the Creative Commons Attribution (CC BY 4.0), which permits unrestricted use, distribution, and reproduction in any medium, as long as the original authors and source are cited. No permission is required from the authors or the publishers.

**Persian Abstract****چکیده**

یک راهکار طراحی برای راکتور غشایی با حسگر فوتومتری جریان دار یکپارچه برای پایش غلظت فررات سدیم به صورت لحظه ای توسعه یافته است. مواد بدنه، حسگر و آندهای مصرفی انتخاب شده اند و پارامترهای بهینه الکترولیز تعیین شده اند که افزایش بازده و غلظت فررات سدیم را با کاهش مصرف انرژی و عملکرد پایدار تا ۸ ساعت تضمین می کنند. تجهیزات توسعه یافته و معرف تولید شده در پساب تصفیه خانه های چاه های نفتی میدان یوزنو-پریوبسکویه در شرایط قطب شمال آزمایش شده اند. در یکی از سایت ها، فررات مستقیماً به آب پساب تزریق شده و سپس رسوب گذاری و فیلتراسیون انجام گرفت، و در سایت دیگر در یک سیستم جامع شامل هوادهی مقدماتی و فیلتراسیون چندمرحله ای به کار رفت. آزمایش های میدانی کارایی بالای فررات سدیم را به عنوان اکسیدکننده، منعقدکننده و لخته کننده نشان دادند؛ تجزیه ترکیبات آلی و سمی، حذف فرآورده های نفتی و ضد عفونی آب حاصل گردید. پس از تصفیه، پارامترهای پساب مطابق با استانداردها بوده و امکان تخلیه ایمن به محیط زیست فراهم شد. نتایج به دست آمده امکان استقرار تجهیزات خودکار و تطبیقی برای سنتز فررات سدیم در سیستم های تصفیه آب در مراکز نفتی را تأیید می کنند. استفاده از فررات سدیم موجب افزایش کارایی تصفیه، کاهش هزینه های بهره برداری و بهبود شاخص های زیست محیطی فرآیندهای تولید می شود.